Published in final edited form as:
J Pharmacol Exp Ther. 2008 October ; 327(1): 32–37. doi:10.1124/jpet.108.141093.

Targeting of VX2 Rabbit Liver Tumor by Selective Delivery of 3-Bromopyruvate: A Biodistribution and Survival Study

Mustafa Vali, **Josephina A. Vossen**, **Manon Buijs**, **James M. Engles**, **Eleni Liapi**, **Veronica Prieto Ventura**, **Afsheen Khwaja**, **Obele Acha-Ngwodo**, **Ganapathy Shanmugasundaram**, **Labiq Syed**, **Richard L. Wahl**, and **Jean-Francois H. Geschwind**
Russell H. Morgan Department of Radiology and Radiological Sciences, Johns Hopkins Hospital, Baltimore, Maryland

Abstract

The aim of this study was to determine the biodistribution and tumor targeting ability of ^{14}C-labeled 3-bromopyruvate ([^{14}C]3-BrPA) after i.a. and i.v. delivery in the VX2 rabbit model. In addition, we evaluated the effects of [^{14}C]3-BrPA on tumor and healthy tissue glucose metabolism by determining ^{18}F-deoxyglucose (FDG) uptake. Last, we determined the survival benefit of i.a. administered 3-BrPA. In total, 60 rabbits with VX2 liver tumor received either 1.75 mM [^{14}C]3-BrPA i.a., 1.75 mM [^{14}C]3-BrPA i.v., 20 mM [^{14}C]3-BrPA i.v., or 25 ml of phosphate-buffered saline (PBS). All rabbits (with the exception of the 20 mM i.v. group) received FDG 1 h before sacrifice. Next, we compared survival of animals treated with i.a. administered 1.75 mM [^{14}C]3-BrPA in 25 ml of PBS (n = 22) with controls (n = 10). After i.a. infusion, tumor uptake of [^{14}C]3-BrPA was 1.8 ± 0.2% percentage of injected dose per gram of tissue (%ID/g), whereas other tissues showed minimal uptake. After i.v. infusion (1.75 mM), tumor uptake of [^{14}C]3-BrPA was 0.03 ± 0.01% ID/g. After i.a. administration of [^{14}C]3-BrPA, tumor uptake of FDG was 26 times lower than in controls. After i.v. administration of [^{14}C]3-BrPA, there was no significant difference in tumor FDG uptake. Survival analysis showed that rabbits treated with 1.75 mM 3-BrPA survived longer (55 days) than controls (18.6 days). Intra-arterially delivered 3-BrPA has a favorable biodistribution profile, combining a high tumor uptake resulting in blockage of FDG uptake with no effects on healthy tissue. The local control of the liver tumor by 3-BrPA resulted in a significant survival benefit.

The knowledge that cancer cells rely on increased glycolysis rather than oxidative phosphorylation for survival is known as “The Warburg Hypothesis” (Warburg, 1956). This concept constitutes the basis for using glycolysis and its associated enzymes as targets for the development of new anticancer therapeutic agents (Shaw, 2006; Gatenby and Gillies, 2007). In our previous studies, we showed that 3-bromopyruvate (3-BrPA) acts as an irreversible inhibitor of metabolic enzyme(s) associated with glycolysis (Ko et al., 2001; Geschwind et al., 2002). Furthermore, we established the therapeutic dose [1.75 mM in 25 ml of phosphate-buffered saline (PBS) and optimal method of delivery (continuous i.a. infusion for 1 h)] of 3-BrPA in a rabbit VX2 model of liver cancer based on pathology (Vali et al., 2007). However, the impact of this treatment strategy on animal survival remains unknown. This information is critical to further develop this approach to the clinic.

Address correspondence to: Dr. Jean-Francois H. Geschwind, Russell H. Morgan Department of Radiology and Radiological Sciences, Division of Vascular and Interventional Radiology, 600 North Wolfe St., Blalock 545, Baltimore, MD 21287. jfg@jhmi.edu.
M.V., J.A.V., and M.B. contributed equally to this work.

Transarterial therapy is one of the most frequently used locoregional treatment options in patients with hepatocellular carcinoma (Georgiades et al., 2001). The main advantage of transarterial delivery of anticancer agents over systemic chemotherapy is the fact that these agents are not infused i.v. throughout the systemic circulation but rather administered locally via the hepatic artery. Thereby, the concentration of the agent within the tumor tissue can be 10 to 100 times higher after i.a. delivery than after systemic delivery (Egawa et al., 1990; Konno, 1990). Because i.a. delivery of 3-BrPA is more complex than the more classic systemic administration, a thorough evaluation of the expected advantages should be made, thereby justifying a detailed pharmacokinetic and biodistribution analysis.

A recent study demonstrated that ^{18}F-deoxyglucose (FDG)-positron emission tomography (PET) can be a useful modality for the early evaluation of the antitumor effect of i.a. administration of 3-BrPA in VX2 liver tumor (Park et al., 2007). The use of PET with the glucose analog FDG is based on the recognition that tumor cells have an increased glucose metabolism (Wagner, 1993; Bomanji et al., 2001). Increased FDG uptake is considered to be indicative of the presence of a metabolically active tumor, whereas lack of FDG uptake indicates tumor cell death.

The aim of this study was to determine and compare the biodistribution as well as tumor targeting ability of ^{14}C-labeled 3-BrPA ([^{14}C]3-BrPA) delivered either i.a. or i.v. delivery in the VX2 model of liver cancer. In addition, we evaluated the effects of [^{14}C]3-BrPA on tumor and healthy tissue glucose metabolism by determining FDG uptake. Last, we determined the survival benefit of intra-arterially administered 3-BrPA in the rabbit VX2 model of liver cancer.

Materials and Methods

Study Design

Two distinct experiments were carried out. The first experiment (n = 60) was designed to assess the biodistribution profile of [^{14}C]3-BrPA and to monitor its influence on FDG uptake. The second experiment (n = 32) was designed to document the survival benefit of 3-BrPA by comparing survival of animals treated with 3-BrPA (n = 22) to controls (n = 10).

Tumor Model

The study was approved by the Animal Care Committee of Johns Hopkins University (Baltimore, MD) and in compliance with institutional guidelines. Adult New Zealand White rabbits weighing 8 to 9 pounds (n = 92; Myrtle's Rabbitry, Thompson Station, TN) were used for this study. For successful implantation of the VX2 tumor into the liver, the tumor was first grown for 2 weeks in the hind leg of a carrier rabbit. Each carrier rabbit was used for implantation into the left lobe of the liver of six rabbits. Before tumor implantation all rabbits were anesthetized with a mixture of acepromazine (2.5 mg/kg; Phoenix, St. Joseph, MO) and ketamine hydrochloride (44 mg/kg; Phoenix) administered i.m.; intravenous access was gained via a marginal ear vein, and sodium pentobarbital (Abbott Laboratories, Abbott Park, IL) was given to maintain anesthesia. VX2 tumor excised from a carrier rabbit was minced and injected into the left lobe of the liver using a 21-gauge angiocatheter. The tumor was allowed to grow for 14 days in all rabbits before treatment was initiated.

Intra-Arterial Delivery Protocol

The induction and maintenance of anesthesia were carried out as described above. Transcatheter hepatic artery infusion of 3-BrPA was performed under fluoroscopic guidance. The animals were brought to the angiography suite and intubated by using a 3.0-mm endotracheal tube (Mallinckrodt Medical, St. Louis, MO) but not ventilated. Surgical cutdown was performed to gain access into the right common femoral artery, after which a 3-French

sheath (Cook, Bloomington, IN) was inserted. A 2-French JB1 catheter (Cook) was manipulated into the celiac axis, after which a celiac arteriogram was obtained to delineate the blood supply to the liver and confirm the location of the tumor. The tumor could readily be visualized as a region of hypervascular blush located on the left side of the liver near the gastric fundus. The left hepatic artery, which provides most of the blood flow to the tumor, was selectively catheterized via the common hepatic artery by using a Transcend guide wire (Boston Scientific, Natick, MA).

After the catheter was adequately positioned within the left hepatic artery, a syringe containing 3-BrPA was connected to the end of the JB1 catheter and carefully placed and adjusted on an infusion syringe pump (Harvard Apparatus model 11 infuse/withdraw single syringe pump; Instech Laboratories, Plymouth Meeting, PA). The infusion rate was set. During the infusion, maintenance of appropriate positioning of the catheter in the hepatic artery was monitored with fluoroscopy. After completion of the infusion the catheter was removed, and the common femoral artery was ligated. All rabbits were monitored during and after the procedure and given analgesics when they showed signs of physical distress.

Radiolabeling

After screening various radioactive markers, we selected carbon-14 as the radiotracer to label 3-BrPA because of its relative ease of synthesis and long half-life. The labeling process consisted of incorporating carbon-14 into pyruvate at the first carbon atom resulting in [1-^{14}C]pyruvate, which was then reacted with elemental bromine leading to the synthesis of [^{14}C]3-BrPA. The radiolabeled analog was purified using normal-phase high-performance liquid chromatography column. The radiochemical purity of the formulated product was determined using analytical high-performance liquid chromatography performing four separate infusions: 1) unlabeled 3-BrPA standard; 2) unlabeled 3-BrPA standard plus [^{14}C]3-BrPA, to demonstrate coelution; 3) [^{14}C]3-BrPA alone; and 4) unlabeled 3-BrPA standard to demonstrate that the retention time for the product has not changed. The chemical purity was >95%. [^{14}C]3-BrPA (15 mCi/mmol) was synthesized at PerkinElmer Life and Analytical Sciences (Waltham, MA). The chemical structure and the position of the ^{14}C label are shown in Fig. 1.

In Vivo Biodistribution Studies

Biodistribution studies were performed in 60 rabbits, 14 days after tumor implantation. Fifty-four rabbits were divided into three groups of 18 animals each. Group 1 was treated i.a. with a 1.75 mM mixture of 100 μCi of [^{14}C]3-BrPA and 3-BrPA in 25 ml of PBS, group 2 received i.v. infusion with a 1.75 mM mixture of 100 μCi of [^{14}C]3-BrPA and 3-BrPA in 25 ml of PBS, and group 3 received i.v. infusion with a 20 mM mixture of 100 μCi of [^{14}C]3-BrPA and 3-BrPA in 25 ml of PBS. Each group was further subdivided into six groups of three rabbits each, corresponding to various time points of sacrifice (0, 30, 60, 120, and 240 min and 24 h after the end of the infusion). Intravenous infusions were given as a continuous infusion over 1 h through a marginal ear vein (infusion rate 25 ml/h). Intra-arterial infusions were given as a continuous infusion over 1 h directly in the left hepatic artery, using the technique described above (infusion rate 25 ml/h). Control rabbits (n = 6) received a 1-h i.v. (n = 3) or i.a. (n = 3) infusion of 25 ml of PBS.

All rabbits, except 18 rabbits in group 3, received 1 mCi of FDG (0.22 mCi/kg) via an ear vein 1 h before sacrifice. After sacrifice, blood, normal tissues (brain, heart, lung, liver, kidney, spleen, stomach, transverse colon, and skeletal muscle) and tumor samples were obtained from each rabbit. The tissue samples were weighed, and FDG uptake was evaluated using a gamma counter (LKB Wallac, Little Chalfont, Buckinghamshire, UK). To correct for radioactive decay

and permit calculation of the concentration of radioactivity in each organ as a fraction of the administered dose, aliquots of the injected dose (ID) were counted simultaneously.

Subsequently, the samples were transferred to scintillation vials, dissolved in 1 ml of Solvable solution (PerkinElmer Life and Analytical Sciences), and color-treated with hydrogen peroxide. After adding scintillation fluid (10 ml) (Ultima Gold; PerkinElmer Life and Analytical Sciences), the sample cpm were counted using a liquid scintillation counter. The percentage of injected dose per gram of tissue (%ID/g) was calculated using the cpm.

Survival Study

Survival studies were performed in 32 animals. Rabbits were divided into three groups; study group 1 (n = 19) and a control group (n = 10), all treated 14 days after tumor implantation in the liver, and study group 2 (n = 3), treated 7 days after tumor implantation. Animals in the study groups (n = 22) were treated witha1h i.a. infusion of 1.75 mM 3-BrPA in 25 ml of PBS, whereas animals in the control group (n = 10) received a 1-h i.a. infusion of 25 ml of PBS. All rabbits were examined daily for appetite, bowel and bladder function, level of activity, and tumor growth. Ten months after treatment or when animals became moribund, failed to eat and drink for more than 3 days, had weight loss >20%, and displayed apathetic behavior, rabbits were sacrificed.

Histological Analysis

All animals in the survival study were euthanized under deep anesthesia by slow injection of a lethal dose (100 mg/5 ml) of sodium pentobarbital i.v. Immediately after euthanasia, liver, lungs, heart, liver, spleen, and kidneys were removed and weighed. Multiple biopsy specimens from the tumor, lungs, heart, liver, spleen, and kidneys, were fixed in formalin, embedded in paraffin, stained with hematoxylin and eosin, and evaluated with a light microscope.

Statistical Analysis

Data were analyzed by use of SPSS for Windows, version 10.0 (SPSS Inc., Chicago, IL). Continuous parameters are reported as mean ± S.D. The data for the treatment groups (%ID/g) were compared. Differences between groups were tested with the two-sample t test. Median survival was calculated from the date of tumor implantation until death. A Kaplan-Meier curve was generated. A p value of less than 0.05 was considered statistically significant.

Results

Biodistribution and Tumor Uptake

The detailed biodistribution data of [^{14}C]3-BrPA at 0 min, 30 min, 60 min, 120 min, 240 min, and 24 h after infusion in VX2 liver tumor-bearing rabbits are shown in Table 1 (i.a. infusion) and Table 2 (i.v. infusion of 1.75 mM). After i.a. infusion, tumor uptake of [^{14}C]3-BrPA was 1.8 ± 0.2, 0.7 ± 0.4, 0.5 ± 0.1, and 0.1 ± 0.03% ID/g at 0 min, 30 min, 120 min, and 24 h, showing tumor retention of the [^{14}C]3-BrPA. Radioactivity levels in the blood were 0.12 ± 0.01% ID/g at 0 min after infusion, followed by a rapid clearance by the end of 240 min (0.03 ± 0.02% ID/g). Selective tumor targeting resulted in a tumor-to-blood ratio of 15.0 at the end of the infusion, which dropped to 3.4 120 min after infusion, but due to rapid blood clearance increased to 20.9 240 min after infusion. Uptake of [^{14}C]3-BrPA in the nontumorous liver was consistently low, ranging from 0.31 240 min after infusion to 0.09 24 h after infusion. Excluding the liver, only the kidneys displayed any appreciable retention of radioactivity. There was very little radioactive retention in the remaining tissues. Uptake of [^{14}C]3-BrPA in the brain was consistently low, with a maximum of 0.009 ± 0.006% ID/g 60 min after infusion.

After i.v. infusion (1.75 mM), tumor uptake of [^{14}C]3-BrPA was significantly lower than after i.a. infusion, measuring 0.03 ± 0.01, 0.04 ± 0.01, 0.05 ± 0.03, and 0.03 ± 0.02% ID/g at 0 min, 30 min, 120 min, and 24 h, respectively. Radioactivity levels in the blood were 0.05 ± 0.01% ID/g at 0 min after infusion, which remained stable over 24 h. Intravenous infusion resulted in a tumor-to-blood ratio of 0.6 at the end of the infusion, which increased to a peak value of 1.3 at 60 min after infusion, a value that is 16 times lower than the peak value after intra-arterial administration. Normal tissue uptake of [^{14}C]3-BrPA was highest in the kidneys, reaching a peak value of 0.16 ± 0.02 at 120 min after infusion.

Intravenous administration with the higher dose (20 mM) did not show any significant difference in biodistribution compared with the lower dose (1.75 mM). Tumor uptake of [^{14}C]3-BrPA was 0.05 ± 0.01, 0.03 ± 0.02, 0.07 ± 0.05, and 0.02 ± 0.01% ID/g at 0 min, 30 min, 120 min, and 24 h. Tumor uptake of [^{14}C]3-BrPA in all groups is shown in Fig. 2.

Influence of intra-arterial and intravenous infusion of [^{14}C]3-BrPA on FDG tumor uptake compared with controls are shown in Fig. 3. Immediately after i.a. administration of [^{14}C]3-BrPA tumor uptake of FDG was 26 times lower compared with tumor uptake of FDG in control animals. This ratio reached a peak of 33 at 30 min after infusion and slowly declined to 2 at 24 h after infusion. However, after i.v. administration of [^{14}C]3-BrPA, there was no significant difference in tumor uptake of FDG compared with control animals.

Survival

Rabbits treated with 1.75 mM i.a. 3-BrPA survived significantly longer than the animals in the control group (Fig. 4). The mean survival time in the control group was 18.6 days, whereas the mean survival time in the treatment group was 55.0 days, showing a statistically significant 296% increase in survival for the rabbits treated i.a. with 3-BrPA ($p < 0.001$).

Histopathologic analysis of the liver in treated animals showed, that their primary liver tumors had not grown from baseline and were mostly necrotic (Fig. 5). Furthermore, the surrounding healthy liver tissue showed no signs of toxicity (Fig. 6). In contrast, histopathologic analysis of the liver in control animals showed near complete replacement of liver parenchyma by tumor with direct extension into adjacent tissues such as the diaphragm and lungs. When examining the extent of tumor dissemination, we observed widespread metastases in the peritoneum, stomach, intestine, and lung in both control and treated animals, indicating that by the time of i.a. treatment the tumor had already spread to extrahepatic sites. The cause of death in the 3-BrPA-treated animals was attributed to the presence of extrahepatic disease, especially in the lungs.

To address this issue, a subgroup of three animals was treated earlier in their disease, i.e., 1 week after tumor implantation mimicking earlier stage liver cancer in humans. One of three animals showed no evidence of recurrence and was considered cured 10 months after treatment. When the liver was excised at the time of sacrifice, a small (less than 1 cm) calcified lesion was present at the site of the tumor, confirming complete tumor destruction. The other two animals did die approximately 80 days after implantation but as with the other animals with advanced liver cancer, they died of respiratory failure due to the presence of lung metastases.

Discussion

Hepatic arterial therapies have become the mainstay of therapy for patients presenting with unresectable hepatocellular carcinoma (Bruix and Sherman, 2005; Del Pozo and López, 2007). The rationale for hepatic arterial chemotherapy is that the infusion of cytotoxic drugs directly into the artery feeding the tumor will maximize tumor concentration and minimize systemic toxicity. In a previous study, we showed that i.a. delivered 3-BrPA in a concentration

of 1.75 mM resulted in complete tumor death (Vali et al., 2007). Because i.a. drug delivery is more complex than the classic systemic administration, a pharmacokinetic and biodistribution analysis was appropriate. Therefore, the first aim of our study was to evaluate the biodistribution of i.a. delivered [^{14}C]3-BrPA and to compare its profile with that obtained after i.v. administration.

For the success of an anticancer agent, a high tumor uptake and a high tumor to normal tissue ratio indicating selective targeting is desirable. The data collected in our study showed that i.a. delivery of [^{14}C]3-BrPA resulted in the highest tumor uptake, with a maximum of 1.8% ID/g. In contrast, i.v. administration of [^{14}C]3-BrPA resulted in significantly lower tumor uptake, with a maximum of 0.07% ID/g, even after a 10-fold increase of the dose. This convincingly shows the superiority of i.a. delivery over i.v. administration in achieving high concentrations of [^{14}C]3-BrPA within the tumor. As expected, uptake of [^{14}C]3-BrPA in the liver was higher after i.a. delivery, compared with i.v. delivery. However, liver uptake of i.a. administered [^{14}C]3-BrPA reached a maximum of only 0.3% ID/g. All remaining tissues showed minimal uptake of [^{14}C]3-BrPA after both i.a. and i.v. delivery, with the kidney showing the highest uptake of 0.23% ID/g. A major finding was the consistently low uptake of [^{14}C]3-BrPA in the high metabolic tissue of the brain, indicating that the drug did not cross the blood-brain barrier.

FDG is a glucose analog that accumulates in cells in a velocity that is dependent on the glycolytic rate of the cell (Gallagher et al., 1978; Kumar et al., 2005). In this study, we used FDG to monitor the effects of i.a. and i.v. delivered 3-BrPA on tumor and healthy tissue metabolism. Our study showed that neither i.a. nor i.v. administration of [^{14}C]3-BrPA influenced the glucose metabolism of healthy tissues. However, after i.a. administration, FDG uptake in the tumor was blocked during the first 2 h after administration followed by a slow increase of FDG uptake, comparable with control levels after 24 h. It is interesting to note that this observation may contradict the results of the histopathologic analysis in our survival study, which unequivocally showed that the primary liver tumors had not grown from baseline and were mostly necrotic. A possible explanation is that a few cancer cells remain viable after the treatment with 3-BrPA. These cells could have simply been stunned by the treatment but not killed. Note that this measurement of FDG activity as described in our study is much more sensitive than PET imaging. Isolated viable cells may therefore not be able to generate a signal that could be detected on PET imaging. Another explanation is that these “stunned” cells could indeed be on a way to a certain death but are still able to take up glucose for their energy needs. After i.v. administration, tumor uptake levels of FDG did not differ from uptake in controls. These results clearly indicate selective tumor metabolism targeting of i.a. delivered [^{14}C]3-BrPA, where healthy tissues are being spared and confirms the advantage of the i.a. delivery method.

The uniquely selective targeting properties of 3-BrPA are evident compared with those of other conventional chemotherapeutic agents. One report using ^{14}C-labeled doxorubicin in a mixture with lipiodol in the same VX2 rabbit model showed that almost all of the doxorubicin disappeared from the tumor immediately after infusion. Therefore, targeting of the tumor by doxorubicin could not be achieved (Konno, 1990).

One possible explanation for the lack of effect of i.v. administered [^{14}C]3-BrPA on FDG uptake in the tumor is the lower concentration at the tumor site (maximum 0.05% ID/g). To achieve concentrations of [^{14}C]3-BrPA in the tumor tissue that are similar to those obtained after i.a. administration, a significantly higher dose of i.v. [^{14}C]3-BrPA is required. However, administration of a higher dose may not show a comparably favorable biodistribution profile and result instead in unfavorable systemic side effects.

The second aim of our study was to evaluate the survival benefit of i.a. administered 3-BrPA in rabbits implanted with the VX2 liver tumor. Our experiments were conducted using the already established dose of 1.75 mM in 25 ml of PBS infused i.a. over 1 h. Treated rabbits had a significant increase in survival compared with the control group. This extension of life span by 36 days or 296% provides convincing evidence for 3-BrPA-mediated survival benefit.

Noteworthy is the absence of toxicity to the normal liver on histopathological analysis, which is in keeping with previous data from our laboratory (Vali et al., 2007). Because most liver cancers arise in the background of underlying liver disease (cirrhosis) and liver failure is a major risk of treatment-related morbidity and mortality in patients, this absence of toxicity is of great importance (Fattovich et al., 2004). These data further confirm the selective targeting of 3-BrPA, which is in line with the results of our biodistribution study.

Although the treatment with 3-BrPA was successful at killing the tumor cells, most animals were not cured by this approach. This may be attributed to the natural biology of the VX2 tumor, which is known to be extremely aggressive, fast growing, and rapidly metastasizes to other tissues and organs, especially the lungs (Rous et al., 1952; Georges et al., 1985; Nishizaki et al., 1990). Histopathologic examination showed that the animals did not die from progression of their liver tumors, but rather from the presence of extrahepatic metastases especially in the lungs. This suggests that the locoregional delivery of 3-BrPA was successful in selectively targeting the liver tumor without causing toxicity to the normal liver parenchyma, and controlling its growth within the liver. Unfortunately, it was not successful in preventing metastatic spread of the VX2 tumor outside the liver.

To minimize the risk of metastatic spread, we decided to treat a small number of rabbits (three animals) at an earlier stage of liver tumor development (7 days after implantation) and showed that earlier intervention leads to further improvement in survival. One of the three animals survived more than 10 months after treatment. When this animal was sacrificed, histopathology showed the tumor to be small (less than 1 cm in diameter), densely calcified, and nonviable. Here, despite evidence of success (one cure of three animals) and a clear attempt on our part to treat earlier in the disease process, our results suggest that this animal model is not appropriate to conduct survival studies because the two animals that died did so as a result of lung metastases. It is for this reason that we did not extend this survival study with a larger number of animals.

This survival study demonstrates the potency of 3-BrPA when given i.a. and its ability kill the liver tumor locally. Specifically, a single bolus infusion of 3-BrPA is not sufficient to kill the entire tumor. By administering 3-BrPA for a prolonged period (>1 h) to the tumor, as we demonstrated from the histopathologic standpoint in a previous report, we were able to achieve significant improvement in survival through complete local tumor control. These results therefore support our therapeutic approach.

In conclusion, we have shown that i.a. delivered 3-BrPA has a favorable biodistribution profile, combining a high tumor uptake resulting in direct blockage of FDG uptake with no effects on healthy tissue. Furthermore, i.a. infusion of 3-BrPA in VX2 implanted liver tumors proved to be beneficial because it resulted in significant survival benefit without any treatment related toxicity. These results argue strongly for the initiation of clinical studies to investigate the safety and efficacy of 3-BrPA as a human anticancer drug.

Acknowledgments

J.-F.H.G. was supported by National Cancer Center Grant R01 CA100883-01 and the Abdulrahman Abdulmalik Research Fund.

ABBREVIATIONS

3-BrPA, 3-bromopyruvate; [^{14}C]3-BrPA, ^{14}C-labeled 3-BrPA; PBS, phosphate-buffered saline; FDG, ^{18}F-deoxyglucose; PET, positron emission tomography; ID, injected dose; %ID/g, percentage of injected dose per gram of tissue.

References

Bomanji JB, Costa DC, Ell PJ. Clinical role of positron emission tomography in oncology. Lancet Oncol 2001;2:157–164. [PubMed: 11902566]

Bruix J, Sherman M. Management of hepatocellular carcinoma. Hepatology 2005;42:1208–1236. [PubMed: 16250051]

Del Pozo AC, López P. Management of hepatocellular carcinoma. Clin Liver Dis 2007;11:305–321. [PubMed: 17606209]

Egawa H, Maki A, Mori K, Yamamoto Y, Mitsuhashi S, Bannai K, Asano K, Ozawa K. Effects of intra-arterial chemotherapy with a new lipophilic anticancer agent, estradiol-chlorambucil (KM2210), dissolved in lipiodol on experimental liver tumor in rats. J Surg Oncol 1990;44:109–114. [PubMed: 2162452]

Fattovich G, Stroffolini T, Zagni I, Donato F. Hepatocellular carcinoma in cirrhosis: incidence and risk factors. Gastroenterology 2004;127:S35–S50. [PubMed: 15508101]

Gallagher BM, Fowler JS, Gutterson NI, MacGregor RR, Wan CN, Wolf AP. Metabolic trapping as a principle of oradiopharmaceutical design: some factors responsible for the biodistribution of [18F]2-deoxy-2-fluoro-D-glucose. J Nucl Med 1978;19:1154–1161. [PubMed: 214528]

Gatenby RA, Gillies RJ. Glycolysis in cancer: a potential target for therapy. Int J Biochem Cell Biol 2007;39:1358–1366. [PubMed: 17499003]

Georges E, Breitburd F, Jibard N, Orth G. Two Shope papillomavirus-associated VX2 carcinoma cell lines with different levels of keratinocyte differentiation and transplantability. J Virol 1985;55:246–250. [PubMed: 2409299]

Georgiades CS, Ramsey DE, Solomon S, Geschwind JF. New nonsurgical therapies in the treatment of hepatocellular carcinoma. Tech Vasc Interv Radiol 2001;4:193–199. [PubMed: 11748557]

Geschwind JF, Ko YH, Torbenson MS, Magee C, Pedersen PL. Novel therapy for liver cancer: direct intraarterial injection of a potent inhibitor of ATP production. Cancer Res 2002;62:3909–3913. [PubMed: 12124317]

Ko YH, Pedersen PL, Geschwind JF. Glucose catabolism in the rabbit VX2 tumor model for liver cancer: characterization and targeting hexokinase. Cancer Lett 2001;173:83–91. [PubMed: 11578813]

Konno T. Targeting cancer chemotherapeutic agents by use of lipiodol contrast medium. Cancer 1990;66:1897–1903. [PubMed: 2171752]

Kumar R, Nadig MR, Chauhan A. Positron emission tomography: clinical applications in oncology. Part 1. Expert Rev Anticancer Ther 2005;5:1079–1094. [PubMed: 16336099]

Nishizaki T, Matsumata T, Kanematsu T, Yasunaga C, Sugimachi K. Surgical manipulation of VX2 carcinoma in the rabbit liver evokes enhancement of metastasis. J Surg Res 1990;49:92–97. [PubMed: 2359299]

Park HS, Chung JW, Jae HJ, Kim YI, Son KR, Lee MJ, Park JH, Kang WJ, Yoon JH, Chung H, et al. FDG-PET for evaluating the antitumor effect of intraarterial 3-bromopyruvate administration in a rabbit VX2 liver tumor model. Korean J Radiol 2007;8:216–224. [PubMed: 17554189]

Rous P, Kidd JG, Smith WE. Experiments on the cause of the rabbit carcinomas derived from virus-induced papillomas. II. Loss by the Vx2 carcinoma of the power to immunize hosts against the papilloma virus. J Exp Med 1952;96:159–174. [PubMed: 14955572]

Shaw RJ. Glucose metabolism and cancer. Curr Opin Cell Biol 2006;18:598–608. [PubMed: 17046224]

Vali M, Liapi E, Kowalski J, Hong K, Khwaja A, Torbenson MS, Georgiades C, Geschwind JF. Intraarterial therapy with a new potent inhibitor of tumor metabolism (3-bromopyruvate): identification of therapeutic dose and method of injection in an animal model of liver cancer. J Vasc Interv Radiol 2007;18:95–101. [PubMed: 17296709]

Wagner HN Jr. Oncology: a new engine for PET/SPECT. Highlights of the Society of Nuclear Medicine annual meeting. J Nucl Med 1993;34:13N–16N. 19N, 22N–29N.

Warburg O. On the origin of cancer cells. Science 1956;123:309–314. [PubMed: 13298683]

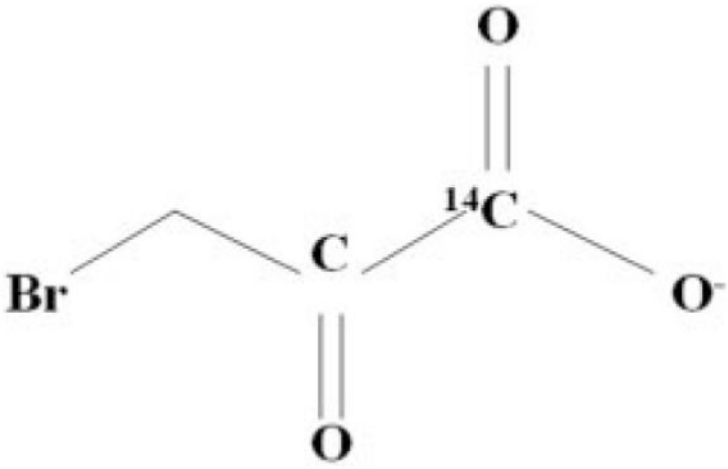

Fig. 1.
The chemical structure of [^{14}C]3-BrPA with the position of the ^{14}C label.

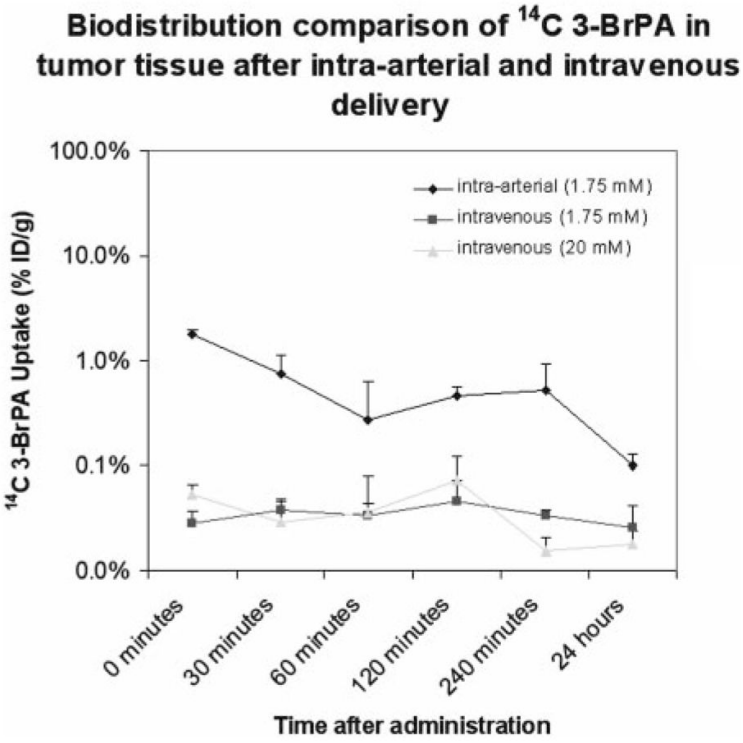

Fig. 2.

Comparison of [^{14}C]3-BrPA tumor uptake after the end of a 1-h i.a. infusion with a 1.75 mM mixture of 100 μCi of [^{14}C]3-BrPA and 3-BrPA in 25 ml of PBS (infusion rate 25 ml/h); after the end of a 1-h i.v. infusion with a 1.75 mM mixture of 100 μCi of [^{14}C]3-BrPA and 3-BrPA in 25 ml of PBS (infusion rate 25 ml/h); after the end of a 1-h i.v. infusion with a 20 mM mixture of 100 μCi of [^{14}C]3-BrPA and 3-BrPA in 25 ml of PBS (infusion rate 25 ml/h).

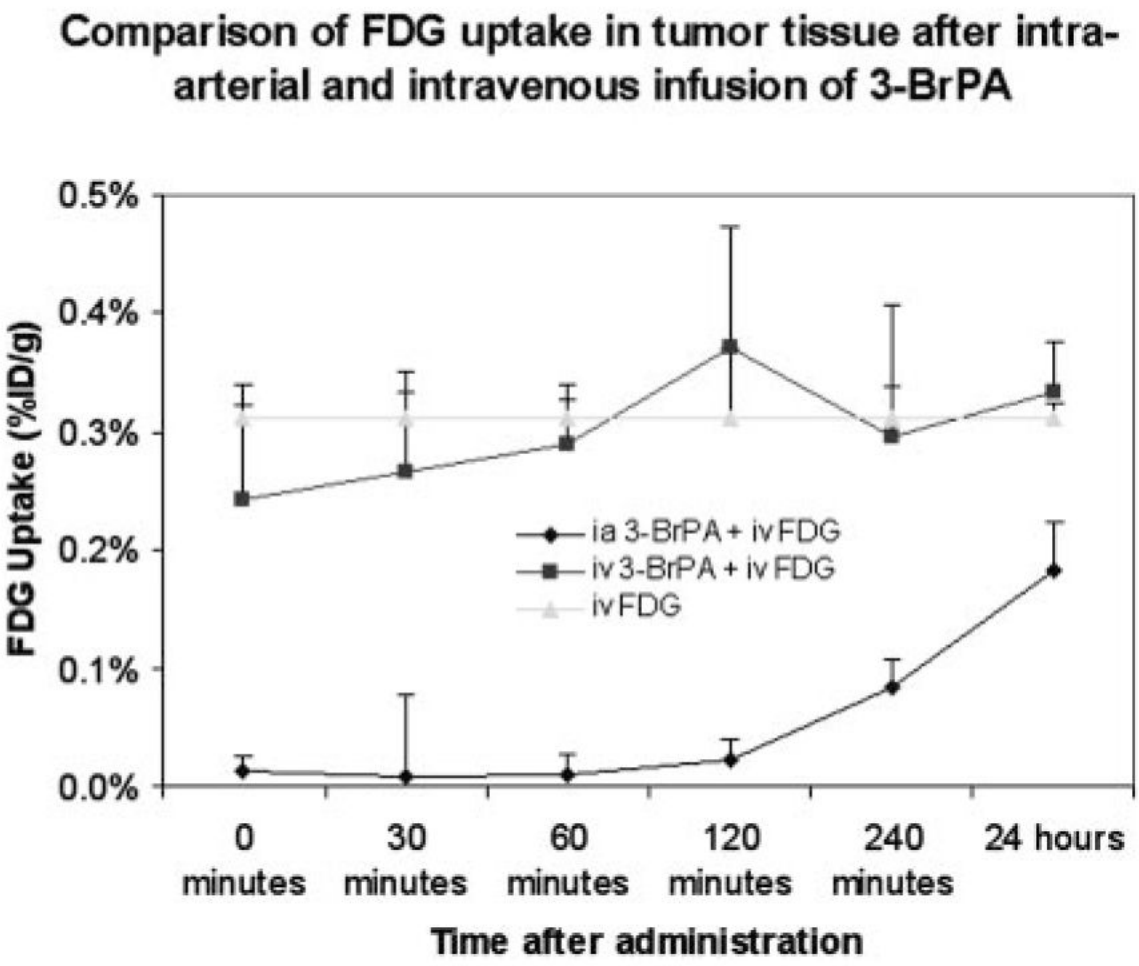

Fig. 3.

Comparison of FDG tumor uptake after the end of a 1-h i.a. (*n* = 18) or i.v. (*n* = 18) with a 1.75 mM mixture of 100 μCi of [^{14}C]3-BrPA and 3-BrPA in 25 ml of PBS (infusion rate 25 ml/h). Control rabbits (*n* = 6) received a 1-h i.v. (*n* = 3) or i.a. (*n* = 3) infusion of 25 ml of PBS. All rabbits received 1 mCi of FDG (0.22 mCi/kg) via an ear vein (i.v.) 1 h before sacrifice.

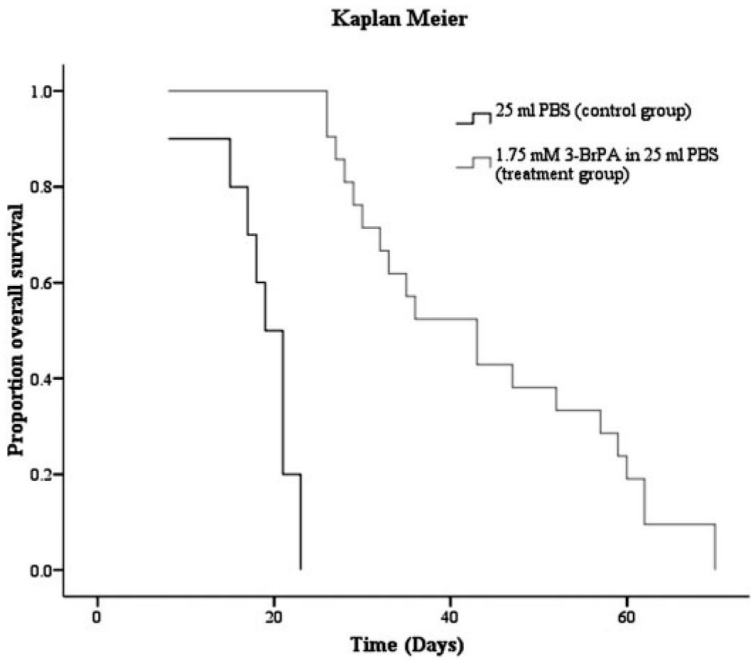

Fig. 4.

Kaplan-Meier survival curves, comparing animals treated with a 1-h i.a. infusion of 1.75 mM 3-BrPA in 25 ml of PBS (n = 22) to control animals treated with a 1-h i.a. infusion of 25 ml of PBS (n = 10).

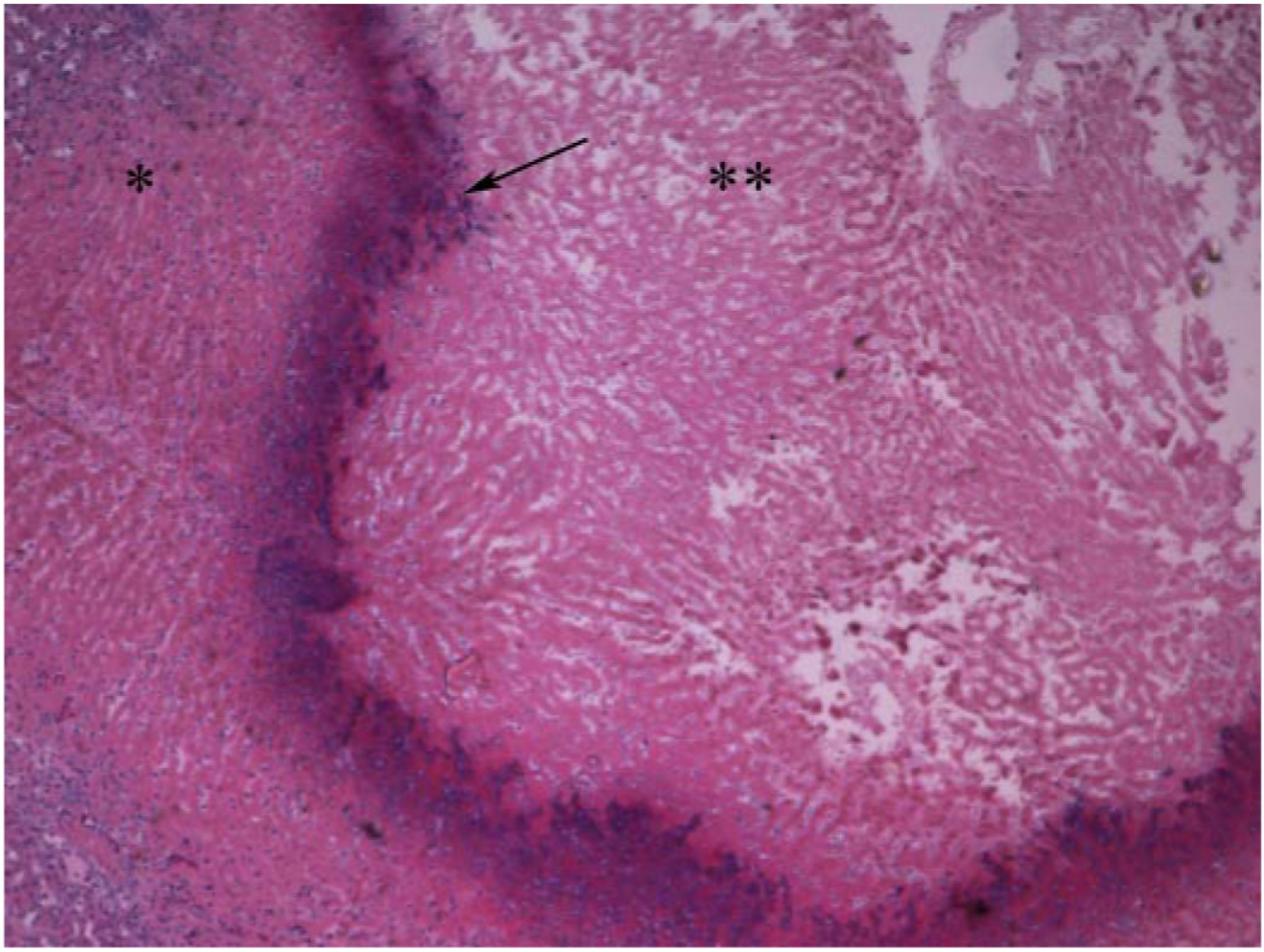

Fig. 5.
Hematoxylin and eosin slide of the tumor (**) and surrounding liver (*) in a rabbit treated with 1.75 mM of 3-BrPA. The tumor has not grown from baseline, is necrotic and encapsulated (arrow).

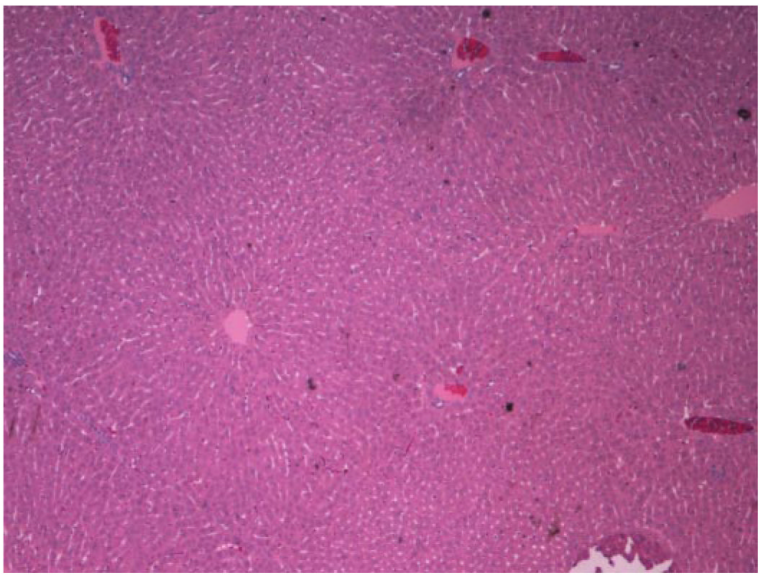

Fig. 6.
Hematoxylin and eosin slide of the liver tissue in a rabbit treated with 1.75 mM of 3-BrPA. The liver tissue shows no signs of toxicity.

TABLE 1

Biodistribution data in 18 animals at 0 min (n = 3), 30 min (n = 3), 60 min (n = 3), 120 min (n = 3), 240 min (n = 3), and 24 h (n = 3) after the end of a 1-h i.a. infusion with a 1.75 mM mixture of 100 μCi of [^{14}C]3-BrPA and 3-BrPA in 25 ml of PBS (infusion rate 25 ml/h)

	% ID (mean ± S.D.) of [^{14}C]3-BrPA in Organ Tissue Samples at Different Time Points after i.a. Administration (1.75 mM)											
	0 min		30 min		60 min		120 min		240 min		24 h	
Blood	0.117	0.013	0.055	0.040	0.066	0.014	0.131	0.087	0.025	0.021	0.016	0.003
Brain	0.006	0.003	0.008	0.002	0.009	0.006	0.007	0.001	0.007	0.004	0.006	0.003
Heart	0.029	0.012	0.044	0.016	0.041	0.028	0.041	0.036	0.030	0.015	0.025	0.024
Lung	0.043	0.006	0.069	0.012	0.053	0.013	0.056	0.018	0.076	0.021	0.026	0.018
Liver	0.115	0.071	0.143	0.072	0.229	0.238	0.290	0.146	0.305	0.230	0.088	0.057
Kidney	0.096	0.031	0.180	0.084	0.143	0.039	0.124	0.056	0.225	0.039	0.056	0.052
Spleen	0.037	0.018	0.045	0.012	0.062	0.028	0.040	0.004	0.055	0.029	0.046	0.045
Stomach	0.024	0.014	0.061	0.019	0.033	0.008	0.052	0.034	0.041	0.012	0.057	0.074
Gastrointestinal tract	0.021	0.003	0.039	0.008	0.041	0.015	0.049	0.033	0.053	0.029	0.022	0.017
Muscle	0.007	0.002	0.031	0.014	0.032	0.018	0.016	0.006	0.014	0.006	0.020	0.018
Tumor	1.781	0.222	0.744	0.391	0.274	0.354	0.452	0.099	0.523	0.405	0.099	0.029

J Pharmacol Exp Ther. Author manuscript; available in PMC 2009 October 12.

TABLE 2

Biodistribution data in 18 animals at 0 min (n = 3), 30 min (n = 3), 60 min (n = 3), 120 min (n = 3), 240 min (n = 3), and 24 h (n = 3) after the end of a 1-h i.v. infusion with a 1.75 mM mixture of 100 μCi [^{14}C]3-BrPA and 3-BrPA in 25 ml of PBS (infusion rate 25 ml/h)

	% ID (Mean ± S.D.) of [^{14}C]3-BrPA in Organ Tissue Samples at Different Time Points after i.v. Administration (1.75 mM)											
	0 min		30 min		60 min		120 min		240 min		24 h	
Blood	0.048	0.011	0.089	0.009	0.026	0.001	0.058	0.005	0.062	0.012	0.038	0.001
Brain	0.034	0.041	0.010	0.006	0.002	0.000	0.002	0.001	0.003	0.000	0.003	0.001
Heart	0.046	0.007	0.042	0.006	0.025	0.003	0.025	0.003	0.022	0.004	0.018	0.006
Lung	0.055	0.011	0.059	0.009	0.046	0.008	0.038	0.003	0.037	0.008	0.025	0.005
Liver	0.073	0.017	0.080	0.003	0.070	0.012	0.059	0.049	0.048	0.022	0.054	0.026
Kidney	0.154	0.015	0.158	0.038	0.143	0.036	0.163	0.022	0.094	0.033	0.040	0.007
Spleen	0.051	0.004	0.045	0.010	0.058	0.035	0.043	0.008	0.034	0.006	0.026	0.006
Stomach	0.037	0.014	0.051	0.016	0.030	0.005	0.046	0.013	0.036	0.017	0.013	0.004
Gastrointestinal tract	0.064	0.062	0.045	0.011	0.024	0.001	0.028	0.006	0.020	0.004	0.018	0.002
Muscle	0.005	0.005	0.023	0.016	0.005	0.001	0.008	0.004	0.005	0.004	0.005	0.001
Tumor	0.029	0.008	0.038	0.008	0.033	0.010	0.045	0.028	0.033	0.005	0.026	0.016